PCCP

RSC Publishing

PERSPECTIVE

View Article Online
View Journal

Developments in understanding and controlling self assembly of DNA-functionalized colloids

Cite this: DOI: 10.1039/c3cp43841d

Lorenzo Di Michele and Erika Eiser*

Received 30th October 2012,
Accepted 8th January 2013

DOI: 10.1039/c3cp43841d

www.rsc.org/pccp

In this article we review the latest achievements in understanding and controlling DNA-mediated interactions between colloidal particles. We report the results of experiments, theoretical studies and computer simulations designed to investigate interactions and aggregation/melting behaviour of DNA-functionalized colloids. The unprecedented insight into the physical effects influencing the interactions and their relation with the tunable parameters of the grafted DNA has resulted in innovative DNA coatings, which are expected to solve the decennial issues encountered in the self assembly of DNA-coated colloids.

1 Introduction

DNA-coated colloids (DNACCs) appeared for the first time in 1996 with two letters published in the same issue of Nature. Alivisatos *et al.*[1] reported a strategy to assemble gold nanocrystals into dimers or trimers *via* base-pairing interactions. Their approach consisted in attaching single-stranded DNA (ssDNA) oligonucleotides to nanocrystals and using double-stranded DNA (dsDNA) to template the oligomerization of the particles. The authors also anticipated that the novel approach could be used to build more complex two or three dimensional constructs. Mirkin and coworkers[2] were the first to demonstrate the reversible aggregation of gold nanoparticles in a composite colloids/DNA material. They used a binary mixture of nanoparticles coated with 2 different ssDNA oligonucleotides and induced aggregation by adding DNA duplexes to link the two strands.

A number of analogous projects were started, triggered by the technological need for tools capable of controlling the assembly of mesoscopic building blocks in complex "metamaterials" with well advertised applications in integrated electronics, photonics, optoelectronics, quantum computation *etc.*[3–5] The Watson–Crick base pairing[6–8] was identified as the perfect candidate for the purpose of controlling aggregation of micro- and nano-objects, due to the high specificity and thermal reversibility of the bonding, the easy production of arbitrary (short) sequences of

Biological and Soft Systems, Cavendish Laboratory, University of Cambridge, JJ Thomson Avenue, Cambridge CB3 0HE, UK. E-mail: ee247@cam.ac.uk

Lorenzo Di Michele

Lorenzo Di Michele studied physics at the University of L'Aqila (Italy), where he also received his Master's Degree. Since 2010 he is PhD student at the Cavendish Laboratory (University of Cambridge), where he focuses on experimental and simulation studies of colloid self-assembly mediated by (bio)polymers.

Erika Eiser

Dr Erika Eiser is Reader at the Cavendish Laboratory of the University of Cambridge. After studying physics at the University of Konstanz (Germany) she received her PhD from the Weizman Institute, Israel, in soft matter physics. Following post-doctoral research at the University of Montpellier and the ESRF in Grenoble (France), she joined the science faculty of the University of Amsterdam as Assistant Professor, where she started developing strategies to drive DNA-driven self-assembly of colloids using various microscopy methods. Her group continues this work in Cambridge.

nucleotides and the possibility of grafting DNA strands to solid materials.

The initial enthusiasm about this new self-assembly frontier slowly faded. It was indeed relatively straightforward to induce aggregation of DNA coated colloids in amorphous, fractal-like phases, but the goal of growing ordered structures, and most important, to engineer them *a priori* by changing the properties of the DNA coating, turned out to be challenging.

Physical intuition borrowed from atomic and molecular physics invited many to think that colloids coated with complementary DNA strands, like any other particles interacting through attraction, would eventually arrange in crystalline phases by minimizing the systems free energy. The above intuition may be correct, but two crucial aspects need to be considered, both following from the complexity of super-molecular systems with a large number of degrees of freedom.

The first aspect is kinetics. Even if in suitable conditions a DNA mediated attraction would drive colloidal particles into a thermodynamically stable crystalline phase, any pathway to reach this state starting from a colloidal gas will encounter metastable free-energy minima, slowing down equilibration dramatically. The two main reasons for this phenomenon are the strength of the attraction and the sharp thermal activation of the aggregation process.[9–14] Several strategies have been attempted or suggested to go around such kinetic barriers, for instance by reducing the strength of the attraction by including inert polymers (*i.e.* double-stranded DNA) in the coating.[10,11,15] The most successful strategy, however, consists in using small nanoparticles (NPs) instead of micron-sized colloids. The obvious advantages are the weaker intercolloid attraction (due to the fewer strands per colloid), the broader aggregation/melting transition, and the increased mobility of the NPs themselves. Systematic crystallization of single-component[16,17] and binary systems[16,18–22] of DNA coated NPs has been achieved by different groups. In contrast, there are much fewer examples of successful crystallization of micron-sized colloids.[15,23,24]

The second aspect that one should consider is that the strength, range, and temperature dependence of DNA mediated interactions are related in a non-trivial way to the tunable parameters of the system, such as the DNA-hybridization free energy, coating density, or strand length, for instance. Early experimental attempts to achieve ordered structures relied on guess-and-check methods for the design of the system, resulting in a list of empiric and poorly understood design rules. In the last few years, however, a number of theoretical and computer-simulation groups devoted large efforts to provide the tools to disentangle different contributions to the overall interactions between DNACCs.[10–14,25–36]

In this perspective we review the latest achievements in understanding and controlling the association–disassociation behavior of DNACCs. We largely focus on theoretical models and computer-simulation studies, which currently represent the hottest area of investigation, but also summarize up-to-date experimental results.

The remainder of the article is structured as follows. In the second section we provide a brief overview of the existing types of DNA coating and binding mechanisms, presenting possible variations on the original idea of ssDNA grafted NPs. In the third sections we describe successful experimental approaches and open issues about the self assembly of DNACCs in ordered phases, highlighting the fundamental differences between nano- and micro-colloids. In the fourth section we describe results from direct experimental measurements of DNA-mediated colloidal interactions, which better clarify the factors limiting the capability of DNACCs to assemble in ordered structures. The fifth, and central section of this paper describes in detail recent theoretical and computational studies of DNA-mediated interactions, with special attention to the case of micron-size particles. At the end of the fifth section we describe how a deeper comprehension allowed an unprecedented control over the interactions between DNACCs, and how this control can be exploited to design ''smarter'' DNA coatings, more suitable to achieve controlled self-assembly in ordered structures. Finally, we summarize the content of the article and give our personal outlook.

2 Overview on DNA coatings

In this section we summarize most of the possible design variations for DNACCs. We do not enter the details of the coating procedures, the readership interested in this aspect may find information in ref. 9 and articles quoted therein.

The original realization of DNACCs made use of gold nanoparticles ($\approx$10–20 nm in diameter) and ssDNA strands of about 10 base-pairs (bp) covalently linked to the surface *via* thiol groups attached to one of the DNA termini.[1,2,16–22,37–40] DNA strands can be also grafted to micron-sized colloids (polymer-based or inorganic). For instance ssDNA can be labeled with amine groups and linked covalently to the surface of polystyrene beads modified with carboxyl groups.[15] Alternatively, ssDNA can be end-functionalized with biotin and grafted to the surface of colloids that carry either neutravidin or streptavidin proteins. The biotin–avidin bond is the strongest non-covalent bond known in nature and guarantees stability in most of the experimental conditions of interest.[10,11,27,41,42] Nonetheless, it is reversible and should be used with care when working at high temperature or with low ionic strength solutions.[43]

Active ssDNA strands that mediate the interaction are referred to as ''sticky ends''. The sticky ends are most often not directly grafted to the surface of the colloids but connected *via* an inert spacer. The spacers could either be made of ssDNA, which must be non-complementary to any other sequence present in the system, or made of dsDNA. The function of the spacers is to increase the volume explored by the active sticky end, thereby facilitating the bonding. Being significantly longer than the persistence length of ssDNA (1.5–3 nm depending on the ionic strength[44]), ssDNA spacers are flexible [see Fig. 1(a)]. On the other hand, dsDNA spacers are usually shorter than the persistence length of dsDNA (about 40 nm[45]). Indeed, they are often modeled as rigid rods [see Fig. 1(b)]. The stiffness of the joint between rigid dsDNA spacers and the surface of the particle can limit the pivoting movement of the spacer. To improve flexibility a short sequence of ssDNA can be added between the dsDNA spacer and the grafting point. Alternatively, the spacer can be grafted to short dangling polymers.[10,11,15,27,36,41,42]

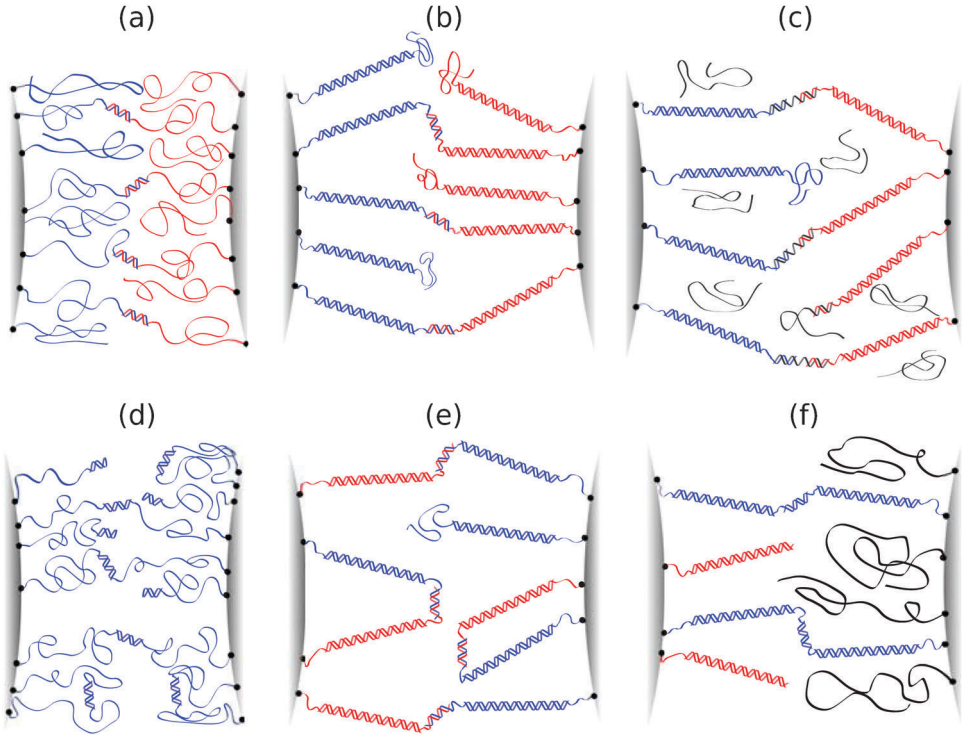

Fig. 1 Schematic of variations on DNA coatings. Each panel shows a detail of the gap region between two approaching colloids. (a) Two different colloids coated with complementary ssDNA. Long non-complementary ssDNA is used as a spacer. (b) Two colloids coated with complementary sticky ends tethered *via* dsDNA rigid spacers. Note that a short ssDNA spacer is left between the dsDNA spacers and the grafting points to improve flexibility. (c) Two colloids coated with non-complementary sticky ends. In this case the bonding is mediated by the ssDNA linkers in solution (black strands). (d) Two identical colloids coated with palindromic sticky ends terminating ssDNA spacers. The sticky ends form hairpins and intra-colloidal loops reducing the number of intercolloidal bridges. (e) Two identical colloids coated with a mixture of dsDNA spacers with complementary sticky ends. The inter-colloid binding competes with the intra-colloid binding. (f) Schematic of two strategies to reduce the attraction by adding dsDNA inert strands (left colloid) or an inert polymer (right colloid).

Aggregation between DNA functionalized colloids can be achieved with a number of different strategies. For instance by taking two species of colloids, one labelled with a ssDNA A and the other labeled with its complementary strand A′. The two species bind directly, as sketched in Fig. 1(a) and (b). An alternative way consists of having the two species coated with non-complementary strands A and B. The linkage is then achieved by adding a third strand in solution (often a DNA duplex), as shown in Fig. 1(c). The advantage of using linkers is the applicability to single-component systems, *i.e.* linkers can be used to bind strands A with strands A.[2,16,17,46,47] The downside is that the linker-mediated binding is a two-step reaction, in which strand A hybridizes with the linker, and only then hybridizes with another non-hybridized strand A. Such a binding scenario is kinetically unfavorable compared to the linker-free approach, which is a one-step reaction. Moreover, the linker-free approach is easier to model and has been used when comparing theoretical predictions and experimental measurements of melting curves and effective potentials.[10,11,27,36,41,42]

An interesting variation of the original linker-free approach consists in using ''palindromic'' or self-complementary sequences.[27,41,42] These strands can either bind to identical strands on a different colloid, forming ''bridges'', or within the same colloid, forming ''loops''. A palindromic strand can also fold on itself and form a ''hairpin''. The formation of hairpins and loops can be controlled by changing the quench rate.[27,41,42] Loops and hairpins reduce the overall number of strands available to form inter-colloid bridges and can therefore be exploited to reduce the strength of the attractive interactions. By using palindromic sequences, it is also possible to achieve aggregation of single-component systems. A cartoon of two colloids interacting *via* palindromic sequences is shown in Fig. 1(d).

A similar coating scheme is shown in Fig. 1(e): Here a mixture of complementary (non-palindromic) strands A and A′ is grafted to the surface of the same colloid. With this design, loops and bridges can form, but hairpins cannot. Analogously to the case of palindromic sequences, one-component systems can aggregate.[27]

Another way to reduce the attractive strength between colloids consists of grafting inert polymers or inert DNA strands together with the active DNA strands[10,11,15,23,27,36,41,42] [see Fig. 1(f)]. The effect is twofold. First, the inert polymers occupy grafting sites on the surface, reducing the grafting density of active strands. Second, the inert polymers cause steric repulsion between the surfaces of two approaching colloids. Both effects can be exploited to engineer the interactions by changing the grafting density and the length of the inert polymers. Mixing the DNA coating with an inert polymer (or double-stranded DNA) brush also helps to reduce non-specific interactions between ssDNA and the bare surface of colloids.[48]

3 Aggregation in ordered phases

In this section we describe experimental realizations of ordered assemblies of DNACCs. Generally, self-assembly experiments are performed by heating up a solution containing all the components (*i.e.* DNACCs and eventual linker sequences) above the melting temperature of the aggregates, then cooling down and incubating at temperatures for which the crystallization is expected to be favorable.

3.1 Nanoscale colloids

As mentioned in the introduction, the main obstacle to the formation of ordered structure is the kinetic arrest of the precursor amorphous phases.

To this end, the use of NPs offers substantial advantages over micron-sized colloids, mainly coming from the smaller number of DNA tethers involved in the interactions. The resultant hybridization mediated attraction presents a (relatively) smooth temperature dependence and is generally weak enough to allow the annealing of the metastable phases within broad temperature intervals. Indeed, relatively simple coating designs can lead to the formation of micron-scale ordered domains with different crystal structures and tunable lattice parameters.[16,19,20,38,47,49]

The first successful experiments involving NPs were reported in the same issue of Nature by Gang and colleagues,[20] and by Mirkin and colleagues.[16] Both groups investigated the aggregation of binary mixtures of nanocolloids in which the interspecies attraction was either produced by complementary sticky ends[20] or by linker duplexes.[16] The binary mixtures crystallized into a body-centered cubic (BCC) structure with CsCl lattice [see Fig. 2(a)].

Mirkin and coworkers also studied a single-component system in which the intra-species attraction was mediated by symmetric duplex linkers.[16] The single-component system crystallized into a close-packed face-centered cubic (FCC) structure [see Fig. 2(b)].

The aggregation was monitored *via* synchrotron based small-angle X-ray scattering (SAXS), which allowed the identification of the crystal phases and the measurement of the lattice parameters.

Mirkin *et al.* found that the unit-cell size depends linearly on the length of the DNA bridges.[46] It was also demonstrated that crystallization is only possible if the ratio between the DNA-bridge length and the nanocolloids diameter is within a given interval.[20,46] In fact, for short DNA strands, the polydispersity of the gold NPs leads to a substantial polidispersity in the effective size of the DNACCs, enough to hinder crystallization. By choosing longer spacers (or linkers) the polydispersity of the gold nuclei becomes negligible compared to the thermal fluctuations of the DNA corona and the crystallization can take place. On the other hand, when very long DNA tethers are used, the crystallization becomes kinetically hindered, most likely because of bonds forming between second neighbors in the amorphous aggregates. The unit cell size was also studied as a function of temperature and found to increase monotonically up to the melting point of the aggregates.[20]

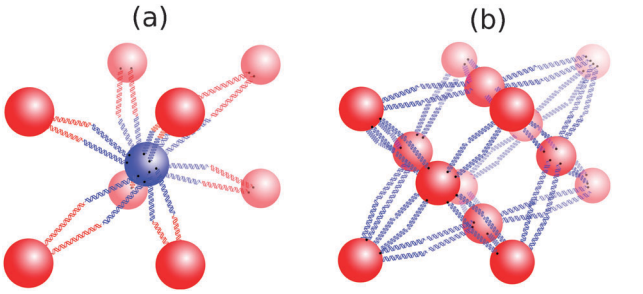

Fig. 2 (a) Sketch of the BCC unit cell into which binary mixtures of DNA-coated NPs with interspecies attraction tend to crystallize. (b) Sketch of FCC unit cell in which single-component mixtures tend to crystallize. For clarity, only bound DNA tethers are shown.

Recently, Mirkin and coworkers[49] reported the results of an accurate study of the crystallization of gold NPs and worked out a set of six empirical rules to determine the structure and the lattice parameter of the crystals as a function of the particle size and the length and number of the DNA tethers. In different conditions, the authors observe the formation of nine distinct crystal structures.

A deeper insight on how tunable physical parameters influence crystallization of DNA coated NPs was provided in recent years by computer simulations.[28,50–60] To simulate a large enough number of colloids, appropriate to extract meaningful informations on phase diagrams, it is necessary to produce coarse grained models for the DNA coatings. For the case of NPs, given the limited number of DNA tethers that can possibly be grafted to them, such models explicitly simulate DNA chains. The same approach is not feasible for the case of micron-size colloids due to the large number of DNA strands involved. For micron-sized colloids, simulations involving explicit DNA strands are only used to calculate pair-interactions,[26,25,29] whereas many-particle simulations usually assume effective pair-interactions between colloids.[25]

One of the most successful coarse grained models for ssDNA coated NPs (or dendrimers) was introduced by Starr, Sciortino and coworkers.[50–54,61] In their model each base of the ssDNA is modeled with two force centers, representing the phosphate–sugar backbone and the nitrogenous base. The backbone sites are connected to each other *via* finitely extensible non-linear springs and the appropriate rigidity of the strand is guaranteed by a three-body bending potential. The bases are connected to the respective backbones and selectively interact with complementary bases *via* Lennard-Jones potentials. Based on this model, Starr and coworkers[50,51] reported a complete molecular dynamics study of the stability of DNA coated NPs crystals upon changing the sticky ends length, the spacer length, the NP size, the number and the rigidity of DNA strands.

De la Cruz and coworkers[60] recently presented a model of DNA-coated gold NPs that allows predictive molecular dynamics simulations. Their model, based on the one introduced by Travesset and coworkers,[59] accurately accounts for the rigidity of dsDNA spacers compared to the flexible ssDNA, and the selectivity and the directionality of hydrogen bonds between

complementary nucleotides. Exploiting this model the authors were able to trace out a quantitative phase diagram and reproduce four out of the nine crystal structures experimentally observed by Mirkin and coworkers.[49]

We also mention the coarse grained model of DNA developed in Oxford.[62,63] With their model the authors succeeded to reproduce a vast range of DNA behavior, including duplex and hairpin formation, as well as structural features such as persistence length and elastic moduli of the duplexes, which will be useful in further refining binding schemes between DNACCs.

Very recently, Frenkel and coworkers,[56] reported a quantitative Monte Carlo study on the phase diagram of a binary mixture of DNA coated NPs based on a newly developed coarse grained model. Their core-blob model treats each DNA sticky end as a soft blob, connected to an effective core, which accounts for the presence of the gold NPs as well as the DNA spacers to which the sticky ends are connected. Compared to the model of Starr and coworkers[50–54,61] or de la Cruz and coworkers,[59,60] this level of coarse graining guarantees a tenfold reduction in the number of degrees of freedom per nanoparticle.

Some aspects of the structure of the DNA-linked NP assemblies are strictly related to molecular level details. Among these, we mention the open questions related to the high-packing of DNA on gold NPs surfaces, an example of which is given by the recent study by Lee *et al.*[64] The authors make use of atomistic level models to investigate the molecular structure of the DNA strands bridging gold NPs.[64–66] Double-stranded DNA can assume different configurations. The most common structure in physiological environment, originally formulated by Watson and Crick,[6] is known as B-DNA. Other forms have been discovered later on. One of them, the A-DNA, is characterized by a thicker double helix structure, which results in a reduced contour length compared to B-DNA strands with the same number of base pairs.

Experimentally, it was observed that the equilibrium distance between DNA-linked gold NPs is too short compared to the length that the dsDNA linkers would assume in the B-DNA form.[16,67] It has therefore been hypothesized that in the particular experimental conditions used in gold NP experiments, *i.e.* high packing density of DNA and high ionic strength, the A-DNA form might be more stable than the B-DNA form. However, fully-atomistic simulations by Lee *et al.*[64] demonstrate that in realistic experimental conditions, B-DNA is more stable than A-DNA, and the shortening of the dsDNA linkers found in experiments can be explained by partial absorption of the DNA to the surface of the NPs.

3.2 Micron-sized colloids

Inducing the self-assembly of micron-sized DNACCs in ordered phases has proven to be much more challenging than for the case of gold NPs. In most cases only amorphous phases form,[15,21,23,68,69] even though a crystal phase is expected to be thermodynamically more stable. The work of Crocker *et al.*[15,23,24] represents one of the few exceptions. They reported the DNA mediated crystallization in close-packed lattices of polystyrene microspheres partially sedimented at the bottom of the sample chambers, *i.e.* in a quasi-2D environment. The authors account the extreme sensitivity of the DNA mediated aggregation process to experimental conditions,[23] such as the DNA coating density, the incubation temperature and the steric repulsion between colloids. In particular, crystallization is only possible if the hybridization-mediated attraction is strong enough to cause clustering, yet weak enough to allow structural rearrangement. The authors estimated that due to the steep temperature dependence of the binding free-energy, suitable conditions for crystallization are only realized within a narrow temperature window of about 0.5 °C.

A less conventional example of DNA mediated colloidal crystallization has been reported by Eiser *et al.*[70–72] In this case, density-matched micron-sized colloids coated with very long dsDNA strands that have some attraction to differently coated surfaces were found to crystallize in 2D hexagonal lattices.

Even in favorable experimental conditions, the formation of microcolloid crystals requires an incubation of several hours, often days, and involves only a very small fraction of the available particles. Moreover, the observed close-packed crystals can be produced much more easily by depletion attraction or simply by entropic crystallization of hard spheres. Also, the construction of photonic band-gap materials, one of the most advertised applications of microcolloids crystals, requires more "open" lattices, for instance the diamond lattice.

4 Measuring the interactions

Once it was clear that the simple assembly strategies that worked for NP assemblies were not sufficient to overcome the difficulties encountered in controlling the aggregation of micron-sized colloids, the efforts of some research groups turned towards the experimental characterization of the DNA mediated interactions, with the purpose of better understanding their dependence on the tunable parameters of the systems. In the following section we discuss the experimental techniques used to measure the DNA-mediated colloidal interactions and quantitatively characterize the aggregation/melting transition of DNACCs solutions.

4.1 Pair potentials between microparticles

Direct measurements of the pair interaction between micron-sized DNACCs have been presented by Crocker and coworkers.[15,34] The measurements were performed by confining two DNACCs in an elongated optical trap obtained by stretching an ordinary optical trap with a cylindrical lens. The two colloids are confined by a weak harmonic potential along the main axis of the trap and a very strong harmonic potential along the perpendicular direction. Once two interacting colloids are placed in the trap, the separation between them is tracked in time with an accuracy of a few nanometers, and a histogram of the separation distribution is produced. The interaction potential is obtained *via* the Boltzmann relation $P(h) \propto \exp[-F(h)/k_BT]$ upon correction for the confining optical-trap potential.[73] Here, $F(h)$ is the Helmholtz free energy, k_B the Boltzmann constant, and T the temperature. Measurements have been performed for the cases of linker-mediated interactions [Fig. 1(c)] and colloids coated with complementary sticky ends [Fig. 1(a) and (b)], using both rigid dsDNA [Fig. 1(b)] and flexible ssDNA spacers

[Fig. 1(a)]. In all cases the interaction curves show a hybridization mediated attraction for $h < 2L$, where h is the surface–surface distance and L is the length of the DNA spacer. A steep repulsive interaction is found for $h < L$, which is caused by the steric repulsion between DNA brushes. Both these contributions will be described in detail in the following sections. The temperature dependence of the interaction curves is also analyzed. As expected the attractive contribution vanishes at high temperatures whereas the steric repulsion is always measured. The shape and temperature dependence of a typical pair potential between micron-sized DNACCs is sketched in Fig. 3(a).

4.2 Melting curves and aggregation kinetics measurements

Direct measurements of aggregation/melting transitions of DNACCs can be achieved by optical imaging of dilute solutions of micron-sized colloids.[10,11,74] The system is left to equilibrate at a constant temperature until a collection of clusters with a stable distribution is formed. The fraction of single colloids f is then measured with basic particle tracking algorithms. To obtain the melting curves, the singlet fraction f is plotted as a function of temperature. The melting temperature T_m of the DNACCs is defined as the temperature at which $f = 1/2$. Measurements have been carried out by Chaikin and coworkers[10,11,74] upon changing the DNA coating density. As sketched in Fig. 3(b), T_m increases when increasing the DNA surface density, whereas the width of the melting/aggregation region decreases slightly. The melting curves of DNACCs measured are much sharper than the ones measured for the same but free ssDNA in solution.

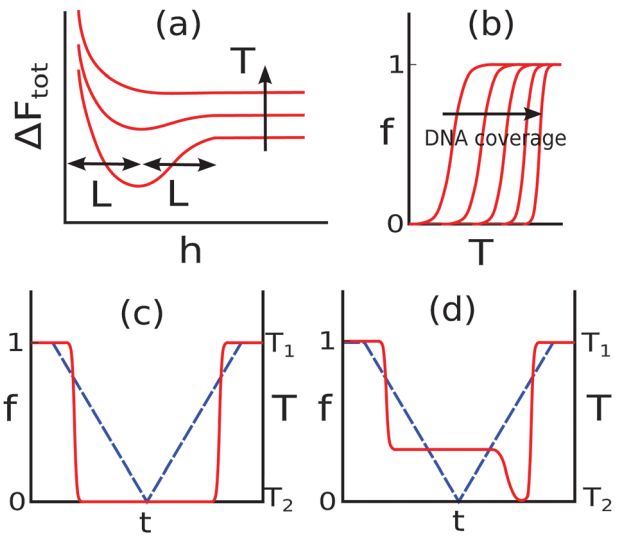

Fig. 3 (a) Sketch of pair interaction between two micron-sized DNACCs coated with complementary strands for different temperatures. (b) Sketch of typical melting curves for micron-sized DNA coated colloids. The melting temperature increases significantly with the DNA coverage whereas the width of the transition decreases only slightly. (c),(d) Fraction of singlets (red solid curves, left axis) as a function of time in a solution of DNA-coated colloids subject to a cooling–heating temperature cycle (blue dashed curves, right axis) for the case of DNACCs coated with (c) simple complementary strands and (d) palindromic sequences.

The same technique has been applied to characterize the aggregation kinetics of micron-sized DNACCs by Leunissen *et al.*[27,41,42] In these experiments the solutions are kept at $T_1 > T_m$, then the temperature is ramped down with a constant rate to $T_2 < T_m$ and finally up again to T_1. The singlet fraction f is monitored during the entire thermal cycle. A typical diagram showing the evolution of f is shown in Fig. 3(c). This technique has been applied by Leunissen and coworkers to study aggregation mediated by complex coatings where inter-colloid bridges compete with the formation of loops and hairpins. For the case of colloids coated with palindromic sequences, in which both loops and hairpins can form, the initial fast aggregation is kinetically arrested when the temperature becomes low enough to make intra-colloid bonds favorable. The faster the quench, the higher the value of f at which the aggregation arrests. When the temperature is raised again above the temperature at which intra-colloid bonds break, colloids start aggregating again because of the new availability of strands to form bridges. Finally, the aggregates melt when the temperature reaches the specific melting temperature of the system. A sketch of the time evolution of f for this particular case is shown in Fig. 3(d).

For the case of nano-sized DNACCs the aggregation/melting transition is monitored using UV-visible absorbance measurements,[12,20] dynamic light scattering[21] or SAXS.[16,20] Generally, the melting aggregation/melting transition of DNA coated NPs was found to be less steep compared to the case of micron-size colloids.

5 Modeling and theoretical predictions

Parallel to the direct measurements of DNA mediated colloidal interactions and DNACCs melting curves, a number of theoretical models have been developed, trying to explain the relation between the tunable parameters of the coatings and the resultant interactions.[10,11,15,25–27,29–36,75] In this section we discuss recently developed techniques to calculate pair-interactions between DNACCs. Such models are especially designed for the case of micron-sized colloids for which, as explained above, an extremely fine control over the interactions is needed to overcome the kinetic issues encountered in self-assembly experiments. The last paragraph of this section will present novel coating strategies expected to (partially) solve such issues.

All the studies reviewed in this section are only concerned with the calculation of pair-interactions, without taking into account many-body effects. It can be proven that if the ratio $R/L > 6.5$, where R is the radius of the particles and L the length of the DNA tether, the interactions are strictly pair-wise additive.[26] This condition is easily fulfilled for the case of micron-size colloids. For nanoparticles, however, DNA tethers can be as long as the diameter of the particles, or even longer. In such situations pair-wise additivity cannot be assumed and the calculation of many-body contributions to the interactions is required for a quantitative description of the aggregation behavior.[56]

The two contributions to the interaction free energy are: (i) the attraction mediated by the hybridization of complementary strands tethered on different colloids, and (ii) the repulsion

due to the compression of the DNA brush between the two surfaces.

The attractive contribution is the most difficult to capture quantitatively and requires a two-step calculation. First, one needs to determine the free energy of hybridization for each pair of interacting tethered sticky ends in the system. This quantity differs from the free energy of hybridization of non-tethered (free in solution) sticky ends. Once the free energy of hybridization for each pair of interacting sticky ends is known, one needs to calculate the overall free energy of interaction between two DNACCs.

5.1 Free energy of hybridization for tethered DNA

We consider two DNA sticky ends i and j grafted *via* inert spacers. The sticky ends can be either grafted to the surface of the same DNACC or to different ones. The hybridization free energy $\Delta G_{ij}^{\mathrm{th}}$ between such strands differs for the same quantity ΔG_{ij}^{0} calculated for sticky ends i, and j freely fluctuating strands in solution. A number of authors[10,11,15,25–27,29,33–36] have presented the derivation of $\Delta G_{ij}^{\mathrm{th}}$ reported below.

The partition function for non-hybridized species i and j and for the hybridized molecule ij, is:

$$Q_X(N_X, V_X, T) = \frac{\Omega_X^{N_X}}{\Lambda_X^{3N_X} N_X!} q_{\mathrm{int},X}^{N_X}, \tag{1}$$

where $X = i, j,$ or ij. N_X is the number of molecules, Ω_X is the available volume in the configurations space, $\Lambda_X = (2\pi\hbar/m_X k_B T)^{1/2}$ is the de Broglie thermal wavelength, m_X is the mass and $q_{\mathrm{int},X}$ is the contribution coming from the internal degrees of freedom. The free energy of hybridization is:

$$\Delta G_{ij}^{\mathrm{th}} = -k_B T \ln\left(\frac{Q_{ij}}{Q_i Q_j}\right). \tag{2}$$

By considering a single pair of sticky ends, *i.e.* $N_i = N_j = N_{ij} = 1$, we have:

$$\frac{Q_{ij}}{Q_i Q_{j'}} = \frac{\Omega_{ij}}{\Omega_i \Omega_j} \frac{q_{\mathrm{int},ij}}{q_{\mathrm{int},i} q_{\mathrm{int},j}} \frac{\Lambda_i{}^3 \Lambda_j{}^3}{\Lambda_{ij}{}^3}. \tag{3}$$

Eqn (2) and (3) can be further simplified. To do so, we consider an equilibrium mixture of freely diffusive sticky ends $i, j,$ and ij. The equilibrium condition requires:

$$\mu_i + \mu_j = \mu_{ij} \tag{4}$$

where $\mu_X = \left(\frac{\partial F_X}{\partial N_X}\right)_{P,T}$ are the chemical potentials and $F_X = -k_B T \ln Q_X$ are the free energies for each component. By using eqn (1) and (4), and assuming that free molecules in solution can explore the same volume $V = \Omega_i = \Omega_j = \Omega_{ij}$ we obtain

$$\frac{q_{\mathrm{int},ij}}{q_{\mathrm{int},i} q_{\mathrm{int},j}} \frac{\Lambda_i{}^3 \Lambda_j{}^3}{\Lambda_{ij}{}^3} = \frac{\rho_{ij}}{\rho_i \rho_j} \tag{5}$$

where $\rho_X = N_X/V$ is the concentration of each component.

The quantity of the left-hand side of eqn (5) can be rewritten in terms of ΔG_{ij}^{0}:

$$\frac{\rho_{ij}}{\rho_i \rho_{j'}} = \frac{\exp\left(-\Delta G_{ij}^{0}/k_B T\right)}{\rho_0} \tag{6}$$

where ρ_0 is a reference concentration. ΔG_{ij}^{0} can be evaluated *via* the nearest-neighbors theory of SantaLucia,[76] or measured experimentally,[10,11] and it can be rewritten separating the enthalpic gain and the entropic penalty of hybridization:

$$\Delta G_{ij}^{0} = \Delta H_{ij}^{0} - T\Delta S_{ij}^{0}. \tag{7}$$

By using eqn (2), (3), (5) and (6), we finally obtain the expression for the free energy of hybridization between the two tethered DNA strands:

$$\Delta G_{ij}^{\mathrm{th}} = \Delta G_{ij}^{0} - k_B T \ln\left(\frac{\Omega_{ij}}{\Omega_i \Omega_j} \frac{1}{\rho_0}\right) \tag{8}$$

We emphasize that by substituting eqn (5) into eqn (3) we have assumed that the internal contributions $q_{\mathrm{int},X}$ are identical for free and tethered molecules. Hence, eqn (8) can be rewritten as:

$$\Delta G_{ij}^{\mathrm{th}} = \Delta H_0 - T\left(\Delta S_0 + \Delta S_{ij}^{\mathrm{conf}}\right). \tag{9}$$

The term $\Delta S_{ij}^{\mathrm{conf}} = k_B \ln\left(\frac{\Omega_{ij}}{\Omega_i \Omega_j} \frac{1}{\rho_0}\right)$ has a purely entropic origin and results from the change in the available volume of the tethered sticky ends before and after hybridization. $\Delta S_{ij}^{\mathrm{conf}}$ goes to zero for $\Omega_{ij} = \Omega_i = \Omega_j = 1/\rho_0$, recovering the result for non-tethered strands.

The dependence of DNACCs interactions on the length and rigidity of the inert spacers is entirely encoded in $\Delta S_{ij}^{\mathrm{conf}}$. For example, we can consider the geometry sketched in Fig. 4, in which the inert spacers are rigid dsDNA rods of length L. The grafting points are assumed to exactly face each other on the surfaces of two DNACCs held at distance h. In this case, the phase-space volumes Ω_X reduce to the volumes V_X accessible to the sticky ends, which are treated as point-like particles:[10,11,27]

$$\begin{aligned} V_i &= V_j = 2\pi L h \quad \text{for } 0 \le h < L \\ V_i &= V_j = 2\pi L^2 \quad \text{for } L \le h < 2L \\ V_{ij} &= 2\pi L \sqrt{1 - \left(\frac{h}{2L}\right)^2} \quad \text{for } 0 \le h < 2L. \end{aligned} \tag{10}$$

The above equations can be generalized to all possible geometries of grafting points, including the case of two strands grafted on

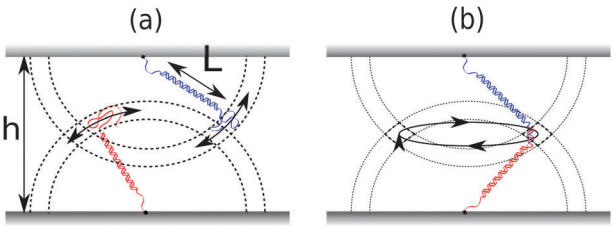

Fig. 4 Configurational space available for (a) non-hybridized and (b) hybridized complementary sticky ends with rigid spacers.

the same colloid.[25–27,33] For the case of sticky ends tethered *via* flexible spacers, Ω_X needs to be calculated *via* Monte Carlo methods.[33]

$\Delta S_{ij}^{\mathrm{conf}}$ depends on the relative grafting position of the strands i and j and not only on the length and rigidity of the spacers. Therefore, it should be calculated for each pair of interacting strands. Alternatively, $\Delta S_{ij}^{\mathrm{conf}}$ can be replaced by an appropriate average or used as a fitting parameter.[10,11]

5.2 Hybridization interaction between colloids

Eqn (9) is the general expression for the free energy of binding of two tethered sticky ends. In this section we describe different strategies for the calculation of the binding free energy ΔF_{att} between two DNACCs grafted with many strands for which the hybridization free energies $\Delta G_{ij}^{\mathrm{hy}}$ are known.

The first approach we present was introduced by Chaikin and coworkers.[10,11,27] This method has the advantage of being analytically tractable to a large extent and to provide physical insight in the nature of the interactions. However, it is based on implicit mean-field assumptions that are only valid for the case of micron-size colloids with high coating densities.

Here we summarize the results obtained for the case of two identical micron-sized colloids uniformly coated with DNA strands carrying complementary sticky ends. A generalization to the case of complex coatings with competing inter-colloid and intra-colloid bonds has been presented by Leunissen *et al.*[27]

Let N_{max} be the maximum number of bridges that can possibly form between the two colloids, and n the average number of possible binding partners for each strand. N_{max} and n can be analytically estimated for the case of micron-sized colloids once the grafting density, the radius of the beads and the length of the rigid dsDNA spacers are known. The partition function of the two interacting colloids can then be written as:

$$\begin{aligned} Z_{\mathrm{att}} &= \sum_{N=0}^{N_{\mathrm{max}}} \binom{N_{\mathrm{max}}}{N} n^N \mathrm{e}^{-N\beta\Delta G^{\mathrm{hy}}} \\ &= \left(1 + n\mathrm{e}^{-\beta\Delta G^{\mathrm{hy}}}\right)^{N_{\mathrm{max}}}, \end{aligned} \tag{11}$$

where ΔG^{hy} is an appropriate average of $\Delta G_{ij}^{\mathrm{hy}}$ over all the involved grafting geometries. ΔF_{att} is then readily computable as:

$$\Delta F_{\mathrm{att}} = -k_{\mathrm{B}}TN_{\mathrm{max}} \ln(1 + n\mathrm{e}^{-\beta\Delta G^{\mathrm{hy}}}). \tag{12}$$

The average number of bridges is also available as:

$$\langle N \rangle = N_{\mathrm{max}} \frac{n\mathrm{e}^{-\beta\Delta G^{\mathrm{hy}}}}{1 + n\mathrm{e}^{-\beta\Delta G^{\mathrm{hy}}}}. \tag{13}$$

ΔF_{att} and $\langle N \rangle$ depend on the distance between the colloids surfaces through the parameters ΔG^{hy}, N_{max} and n. Three regimes can be identified in the eqn (12) and (13): (i) the strong binding regime in which $n\exp(-\beta\Delta G^{\mathrm{hy}}) \gg 1$ and the maximum possible number of bonds is formed, *i.e.* $\langle N \rangle = N_{\mathrm{max}}$; (ii) a weak binding regime for, $N_{\mathrm{max}}n\exp(-\beta\Delta G^{\mathrm{hy}}) \ll 1$, in which the probability of forming even a single bond is low; (iii); an intermediate regime for which the probability of formation of a single bond is low, *i.e.* $n\exp(-\beta\Delta G^{\mathrm{hy}}) \ll 1$, but since the number of possible bonds is very large, *i.e.* $N_{\mathrm{max}} \gg 1$, we still obtain $N_{\mathrm{max}}n\exp(-\beta\Delta G^{\mathrm{hy}}) \gg 1$ and eqn (12) and (13) can be rewritten as:

$$\begin{aligned} \langle N \rangle &= N_{\mathrm{max}} n\mathrm{e}^{-\beta\Delta G^{\mathrm{hy}}} \\ \Delta F_{\mathrm{att}} &= -k_{\mathrm{B}}TN_{\mathrm{max}} n\mathrm{e}^{-\beta\Delta G^{\mathrm{hy}}}. \end{aligned} \tag{14}$$

We note that in the intermediate regime

$$\Delta F_{\mathrm{att}} = -k_{\mathrm{B}}T\langle N \rangle. \tag{15}$$

The intermediate regime is perhaps the most relevant in experiments involving micron-size colloids, and eqn (15) is sometimes erroneously regarded as general.

The partition function in eqn (11) relies on mean-field approximations, namely the assumption that all the N_{max} strands involved in the interaction are equivalent and can interact with n identical near neighbors with the same hybridization free energy ΔG^{hy}. However, such a mean-field approach is only justified for the case of micron-size colloids with a high coating density, and cannot be generalized to the case of poorly grafted colloids or nanoparticles, nor to the case of complex coatings in which the local composition of the coating can fluctuate.

Recently, a more general approach to the modeling of DNA-mediated colloidal interactions has been presented by Varilly *et al.*[33] The authors derived a self-consistent theory that treats independently every strand in the system without mean-field assumptions. Their theory can therefore be applied to DNA coatings of arbitrary complexity as well as to any other valence-limited type of interaction.

Once the hybridization free energy $\Delta G_{ij}^{\mathrm{th}}$ is known for every pair of strands in the system, the partition function can be formally written as:

$$\frac{Z_{\mathrm{att}}}{Z_0} = \sum_{\phi} \prod_{(i,j)\in\phi} \mathrm{e}^{-\beta\Delta G_{ij}^{\mathrm{th}}}. \tag{16}$$

Here, ϕ is a particular configuration of the system corresponding to a list of bound strands (i,j), and Z_0 is the partition function of the reference state in which no strands are bound. We can define Z_{-i} as the partition function of the system for which the strand i is not bound. Analogously, the partition function for which both the strands i and j are not bound is $Z_{-i,-j}$. It follows that $\forall i$:

$$Z = Z_{-i} + \sum_j \mathrm{e}^{-\beta\Delta G_{ij}^{\mathrm{th}}} Z_{-i,-j}. \tag{17}$$

By noticing that $p_i = Z_{-i}/Z$ is the probability of the strand i to be unbound, and by approximating $p_ip_j \approx Z_{-i,-j}/Z$, we can derive a self-consistency condition for p_i from eqn (17):

$$p_i = \frac{1}{1 + \sum_j \mathrm{e}^{-\beta\Delta G_{ij}^{\mathrm{hy}}} p_j}. \tag{18}$$

The above set of equations can be solved iteratively or recast into a minimization problem to calculate the set of p_i.[33] Once the p_i are known, the probability for the two strands i and j to be bound is given by $p_{ij} = p_ip_j\mathrm{e}^{-\beta\Delta G_{ij}^{\mathrm{th}}}$. The attractive free energy between the colloids is then estimated by using

thermodynamic integration.[77] For instance, by introducing the integration parameter λ, such that $\beta\Delta G_{ij}^{\mathrm{hy}} \rightarrow \beta\Delta G_{ij}^{\mathrm{hy}} + \lambda$, we have $Z(\lambda \rightarrow \infty) = Z_0$ and:

$$\begin{aligned}\beta\Delta F_{\mathrm{att}} &= \int_{\infty}^{0} \mathrm{d}\lambda \frac{\partial[-\ln(Z(\lambda)/Z_0)]}{\partial\lambda} \\ &= -\int_{0}^{\infty} \mathrm{d}\lambda \sum_{i<j} p_{ij}(\lambda) = -\int_{0}^{\infty} \mathrm{d}\lambda \langle N(\lambda)\rangle\end{aligned} \tag{19}$$

In a very recent development of the theory, Angioletti-Uberti *et al.*[78] found out the *exact* analytical solution of the integral in eqn (19), which can be expressed as a function of the p_is only. The solution is remarkably simple and can be expressed in a very compact way as:

$$\beta\Delta F_{\mathrm{att}} = \sum_i \ln p_i + \sum_{i<j} p_{ij} = \sum_i \ln p_i + \frac{1}{2}(1 - p_i). \tag{20}$$

Eqn (20) is the result of an ensemble average of an appropriate free-energy functional over all possible bonding configurations of the system.[78] Notably, the saddle point approximation used to calculate this average involves a minimisation procedure, which leads to the same self-consistent equations found in ref. 33. Use of eqn (20) reduces the computational cost with respect to numerical integration by orders of magnitude, extending the practical range of applicability of the theory developed by Varilly and coworkers to very complex and highly inhomogeneous coating scenarios, including the case of mobile linkers. Another important aspect of eqn (20) is that it makes explicit the connection between this theory and previous models found in the literature,[11,15,30,34] such as those leading to eqn (11) and (15); which were shown to be a special, limiting case of the more general eqn (20).

We also mention an alternative approach to the calculation of ΔF_{att} presented by Rogers and Crocker.[34] This method is based on the estimation of $\langle N\rangle$ and relies on eqn (15) to calculate ΔF_{att}. Since eqn (15) is only valid in restricted regimes, the method of Rogers and Crocker suffers from lack of generality compared with the approaches presented above. The authors assume that when two DNACCs coated with complementary sticky ends A and B interact, the fraction of hybridized AB strands can be calculated by modeling the hybridization reaction as a standard equilibrium chemical reaction with non-uniform concentration profiles for the reactants. By designating $\rho_{\mathrm{A}}(\boldsymbol{r})$, $\rho_{\mathrm{B}}(\boldsymbol{r})$, and $\rho_{\mathrm{AB}}(\boldsymbol{r})$ as the equilibrium concentration profiles of the three species, and $\rho_{\mathrm{A}}^0(\boldsymbol{r})$ and $\rho_{\mathrm{B}}^0(\boldsymbol{r})$ as the concentration profile of the unreacted species, we can write the set of equations in the following way:

$$\begin{aligned}\rho_{\mathrm{AB}}(\boldsymbol{r}) &= \frac{\rho_{\mathrm{A}}(\boldsymbol{r})\rho_{\mathrm{B}}(\boldsymbol{r})}{\rho_0} \mathrm{e}^{-\beta\Delta G_{\mathrm{AB}}^0} \\ \rho_{\mathrm{A}}^0(\boldsymbol{r}) &= \rho_{\mathrm{A}}(\boldsymbol{r}) + \rho_{\mathrm{AB}}(\boldsymbol{r}) \\ \rho_{\mathrm{B}}^0(\boldsymbol{r}) &= \rho_{\mathrm{B}}(\boldsymbol{r}) + \rho_{\mathrm{AB}}(\boldsymbol{r})\end{aligned} \tag{21}$$

The last two relations follow from the requirement that the chemical equilibrium condition is fulfilled separately at each position $\boldsymbol{r}$. This approximation has been defined as *local chemical equilibrium* (LCE).[35,36] The profiles of the unreacted species $\rho_{\mathrm{A}}^0(\boldsymbol{r})$ and $\rho_{\mathrm{B}}^0(\boldsymbol{r})$ can be calculated by Monte Carlo techniques for each value of the separation between the two colloids, and the set of eqn. (21) can be solved for $\rho_{\mathrm{AB}}(\boldsymbol{r})$.

Finally $\langle N\rangle$ can be estimated as:

$$\langle N\rangle = \int \mathrm{d}\boldsymbol{r}\rho_{\mathrm{AB}}(\boldsymbol{r}), \tag{22}$$

and the attractive free energy can be calculated using eqn (15). If a single type of linkage is present, the approach of Rogers and Crocker predicts with quantitative accuracy the measured pair-interaction curves for micron- size DNACCs in the intermediate regime. However, the method suffers from two main drawbacks:[35,36] (i) the assumption of LCE requires that the initial concentrations of reactants $\rho_{\mathrm{A}}^0(\boldsymbol{r})$ and $\rho_{\mathrm{B}}^0(\boldsymbol{r})$ are independent of the degree of hybridization, which is only true if the binding probability is very low; (ii) the use of eqn (15) is not general, but only verified if the binding probability is low and the number of possible bonds is large.

5.3 Steric repulsion

The second free-energy contribution in the interaction between two DNACCs is the steric repulsion ΔF_{rep} due to the confinement of DNA, or other polymers grafted to the colloidal surface. At the experimentally relevant coating densities, the DNA–DNA (polymer–polymer, or DNA–polymer) excluded volume is negligible and the confinement is only due to the volume occupied by the partner colloid. The general expression for the repulsive free energy is:

$$\beta\Delta F_{\mathrm{rep}}(h) = -\sum_i \log\left(\frac{\Omega_i(h)}{\Omega_i^0}\right), \tag{23}$$

where the sum runs over all strands in the system. $\Omega_i(h)$ is the configuration-space volume available to the strand i when the distance between the surface of the two colloids is h and Ω_i^0 is the configuration-space volume for the case of isolated colloids. When rigid spacers are used, Ω_i reduces to the volume V_i that is accessible to the sticky end and ΔF_{rep} can be calculated analytically.[10,11,25–27,29,33] By approximating V_i with eqn (10), Dreyfus *et al.*[11] worked out the analytical expression:

$$\begin{aligned}\Delta F_{\mathrm{rep}} &= 2N_{\max}k_{\mathrm{B}}T\ln\left(\frac{L}{h}\right) \quad \text{for } h \le L \\ &0 \quad \text{for } h < L,\end{aligned} \tag{24}$$

which is valid for the case of micron-sized colloids.

For the case of flexible ssDNA spacers, Ω_i can be calculated numerically by exploiting standard techniques in polymer physics.[33,34]

5.4 Predicting melting curves

A number of authors tried to model the melting transition of DNACCs and explain the shift in the melting temperature and the sharpness of the transition found in comparison with melting curves of ssDNA.[10–14,79] Most of the community accepts

that the reasons for these differences are: (i) the entropic contribution to the free energy of hybridization for tethered strands (see eqn (8) and (9)), and (ii) the combinatorial entropy gain following the fact that many strands are involved in the overall interaction. Schatz and coworkers[12–14] also proposed a neighboring-duplex cooperativity mechanism that could sharpen the melting transition of nanoparticles aggregates at high coating densities, *i.e.* when the distance between inter-particle bridges is <5 nm. They suggest that when hybridized DNA duplexes are within a certain distance, the overlap of the ionic clouds surrounding the double helices produces a local increase in the ionic strength. When one or a few of the duplexes de-hybridize, the respective ions are released and free to diffuse away. The remaining duplexes then experience a decrease in the local ionic strength, which triggers their dissociation. However, Lukatsky and Frenkel[79–81] showed that the experimental results of Schatz and coworkers can be explained with entropic cooperativity only, without invoking ion-mediated interactions between duplexes.

In what follows, we briefly discuss the approach presented by Chaikin *et al.*[10,11] to the calculation of the melting curves. The authors worked out an expression for the fraction f of singlets (unbound colloids) within an equilibrium ensemble of 2D DNACCs clusters. The calculation is based on the cell model developed by Sear[82] and gives:

$$f = \frac{1 + 2K\rho - \sqrt{1 + 4K\rho}}{2K^2\rho^2}. \tag{25}$$

In eqn (25), ρ is the overall concentration of colloids and K is the equilibrium constant for the association/dissociation reaction of a single colloid with a cluster. K can be written as:

$$K = \frac{A_w}{\Lambda^4} e^{-\frac{z}{2}\beta\Delta F_{tot}} \tag{26}$$

where z is the average number of nearest-neighbor colloids within a cluster, the parameter A_w is the area within which a bound colloids can wiggle and Λ is a measure of the elementary surface unit of the system. The authors used their analytical expressions for ΔF_{att} (eqn (12)) and ΔF_{rep} (eqn (24)) to fit experimental melting curves with the predictions of eqn (25) by using ΔS^{conf} and A_w as fitting parameters.[10,11] From eqn (25) the melting temperature T_m of DNACCs is also available as the temperature at which $f(T)|_{T_m} = 1/2$. By expanding f as $f(T) \approx f(T_m) + \left.\frac{\partial f}{\partial T}\right|_{T=T_m}(T - T_m)$ we can also extract the width of the melting transition as $\delta {T_m}^{-1} = \left.\frac{\partial f}{\partial T}\right|_{T=T_m}$. Exploiting the analytical description of Chaikin *et al.* it is then possible to understand, which parameters influence T_m and $\delta {T_m}^{-1}$.

Besides the expected dependence of T_m from the coating density, the melting temperature is found to decrease when the configurational entropy of hybridization ΔS^{conf} increases. This allows the possibility of tuning T_m by changing the length of the inert spacers. The behaviour of $\delta {T_m}^{-1}$ is more subtle. For the cases in which few strands are involved in the inter-colloid attractions, *i.e.* the case of nanoparticles or poorly coated microparticles, the melting occurs in the strong binding regime, in which $\langle N\rangle \approx N_{max}$. In this regime $\delta {T_m}^{-1} \propto {N_{max}}^{-1}$, which explains the strong dependence of the melting transition width on the DNA coverage found for nanoparticles. On the other hand, for micron-size DNACCs with high density coatings and many strands involved in the interactions, the melting occurs in the weak binding regime, in which $\langle N\rangle \ll N_{max}$. In this regime $\delta {T_m}^{-1}$ will decrease only slightly upon increasing the coating density (and therefore N_{max}), as found experimentally.[10,11]

5.5 Computer simulations

The most accurate method to calculate pair-interactions between DNACCs is *via* direct Monte Carlo (MC) simulations. The advantage of the computational approach is the applicability to the cases of micro-[25,26,29] and nano-colloids[28,56] with coatings of arbitrary complexity. Here we briefly summarize the MC approach used by Frenkel and coworkers.[25,26,29] The authors consider the case of sticky ends tethered *via* dsDNA spacers. The spacers are modeled as rigid rods of length L freely pivoting around their grafting points and the sticky ends are assumed to be point-like. The grafting points are Poisson-distributed on flat or spherical surfaces at a given average density. The minimum distance between the grafting points is fixed according to the excluded volume of dsDNA.

The interaction energies are calculated for fixed distances between the surfaces of two spheres or flat plates in the range $(0, 2L)$. Each MC move consists of randomly selecting one of the strands i that could be either bound or unbound to a strand j_1. Then, all the possible binding partners $j_1,\ldots,j_n$ are identified and the entropic correction to the hybridization free energy $\Delta S^{conf}_{i,j_k}$ between i and each of the partners is calculated. The hybridization free energies are then $\Delta G^{th}_{i,j_k} = \Delta G^0 - T\Delta S^{conf}_{i,j_k}$, where the hybridization free energy of non-tethered sticky ends ΔG^0 is taken as a constant. The strand i is then bound to a partner j_k with probability:

$$p_{i,j_k} = \frac{\exp\left(-\beta\Delta G^{th}_{i,j_k}\right)}{1 + \sum_{j_l}\exp\left(-\beta\Delta G^{th}_{i,j_k}\right)}, \tag{27}$$

or left unbound with probability:

$$p_{i,j_k} = \frac{1}{1 + \sum_{j_l}\exp\left(-\beta\Delta G^{th}_{i,j_k}\right)}. \tag{28}$$

The average number of bonds $\langle N\rangle$ is sampled and ΔF_{att} is computed by thermodynamic integration[77] using the hybridization free energy of non-tethered sticky ends ΔG^0 as integration parameter:

$$\beta\Delta F_{att} = -\int_{\Delta G^0}^{0} d\Delta G^{0'}\langle N\rangle|_{\Delta G^{0'}}. \tag{29}$$

The repulsive part of the attraction is calculated according to eqn (23).

5.6 Controlling the interactions

The first attempts of rationally designing DNA coatings based on the refined theoretical and computer simulation techniques presented above appeared in literature only very recently.

As stated in the introduction, one of the main obstacles to achieve crystallization of micron-size DNACCs is the kinetic arrest of the aggregates in disordered gel-like phases due to the sharp temperature dependence of the DNA mediated interactions. Indeed, the crystallization of conventional DNACCs turns out to be kinetically allowed only within a narrow temperature window in which hybridization attraction is weak enough to enable structural rearrangements of the aggregates.

Mognetti *et al.*[26] proposed an original strategy to weaken the temperature dependence of the hybridization mediated attraction and potentially broaden the crystallization window. The authors performed computer simulations on a binary mixture of colloids X and X′, each of them coated with two different strands: α and β for colloids X and α′ and β′ for colloids X′. The sticky end α can bind to α′ with a free energy ΔG_{α}^{hy} and to β′ with free energy ΔG_{β}^{hy}. Analogously, the strand α′ can bind to β with the same free energy ΔG_{β}^{hy}. The hybridization of β with β′ is forbidden. The sticky ends are assumed to be grafted *via* rigid dsDNA spacers of length L. The α–α′ bond is stronger compared to α–β′ and α′–β, *i.e.* $\delta\Delta G^{hy} = \Delta G_{\beta}^{hy} - \Delta G_{\alpha}^{hy} > 0$. Therefore, the melting temperature T_{α} of the α–α′ bonds is higher than T_{β}, the one of α–β′ and α′–β. At $T > T_{\alpha}$ none of the bonds can form [see Fig. 5(a)], for $T_{\beta} < T < T_{\alpha}$ only the strong bonds can form [see Fig. 5(b)], and for $T < T_{\beta}$ both strong and weak bonds can form. For each α–α′ bond breaking, two weak bonds can form, consequently, even though at $T < T_{\beta}$ a single strong bond is more favorable than a single weak bond, the system can be designed such that two weak bonds are always more favorable than a single strong one. In this way it is possible to trigger the transition between strong and weak binding when the temperature is lowered below T_{β} [see Fig. 5(c)]. In Fig. 6(a) we sketch the temperature dependence of the number of strong bonds N_{α} and weak bonds N_{β} as a function of temperature. The transition temperature between strong and weak bonds, that is the temperature for which $N_{\alpha} = N_{\beta}$, decreases upon increasing the free energy difference between weak and strong bonds $\delta\Delta G^{hy}$. The strong-to-weak transition also results in a weakening in the temperature dependence of the hybridization mediated attraction between X and X′, as sketched in Fig. 6(b) where the minimum ΔF_{min} of the interaction free energy between X and X′ is plotted as a function of temperature.

Mognetti *et al.* also point out that by using different spacer lengths L_{α} (for α and α′) and L_{β} (for β and β′), combinatorial entropy can be exploited to further enhance the strong-to-weak transition. For example, we can consider a coating in which the grafting densities of α (α′) and β (β′) are equal. By taking $L_{\beta} > L_{\alpha}$, the number of possible β′ (β) binding partners of a single α (α′) sticky end will be larger than the number of α′ (α) partners. In this way the weak bonds can be made entropically more favorable for a fixed $\delta\Delta G^{hy}$.

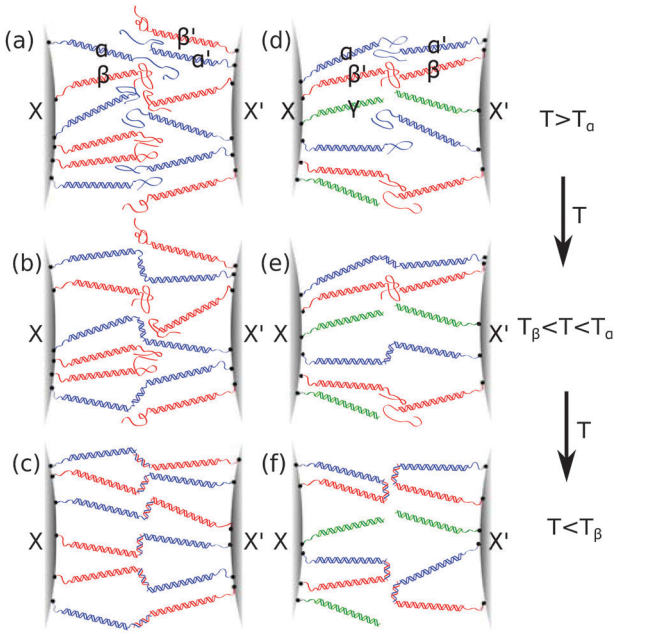

Fig. 5 Cartoon of the surface coatings designs and binding mechanism proposed by Mognetti *et al.*[26] (a)–(c) and by Angioletti-Uberti *et al.*[25] (d)–(f).

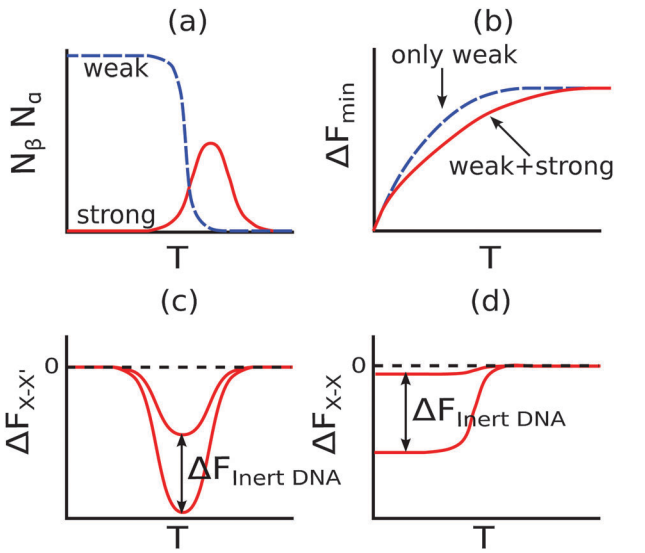

Fig. 6 (a) Qualitative sketch of the temperature dependence of the number N_{α} of strong and N_{β} of weak bonds.[26] (b) Qualitative sketch of the smoothing in the temperature dependence of the DNACCs attraction strength resulting from the competing linkages approach of Mognetti *et al.*[26] Qualitative temperature dependence of the interspecies (c) and intra-species (d) interactions for the binary system designed by Angioletti-Uberti *et al.* The introduction of a fraction of inert strand to the coating causes the interactions to become more repulsive and eventually cancels out the intra-species attraction.

Angioletti-Uberti *et al.*[25,83] demonstrated by computer simulations the possibility of designing a binary mixture of colloids for which the crystallization is even more facilitated. Such a system aggregates only within a specific temperature window, in other words the aggregates can be melted upon cooling as well as heating. The authors combined the competing-linkage

approach[26] with the idea of self-protected interactions proposed by Leunissen and coworkers.[27] They consider a design similar to the one proposed by Mognetti *et al.*,[26] with the only difference that colloids X are coated with strands α and β′, and colloids X′ are coated with α′ and β, as sketched in Fig. 5(d)–(f). In this way, the weak bonds α–β′ and α′–β can occur between strands grafted on the same colloid (loops) as well as on different colloids of the same species. The resulting binary mixture experiences a peculiar temperature dependence of the interspecies (X–X′) and intra-species (X–X or X′–X′) interactions. The interspecies attraction is caused by strong α–α′ bonds and is therefore only active for $T < T_\alpha$ [see Fig. 5(e)]. For $T < T_\beta$ the strong bonds are replaced by weak bonds forming loops within the same colloids or intra-species bridges [see Fig. 5(f)]. Consequently, the X–X′ interaction is attractive in the temperature window between T_α and T_β, as sketched in Fig. 6(c). The magnitude of the inter-species attraction can be arbitrarily increased by increasing $\delta\Delta G^{hy}$. The intra-species interaction is repulsive for $T > T_\beta$, weakly attractive $T < T_\beta$ and saturates to a constant value at low temperatures, as shown in Fig. 6(d). It is however possible to add a third inert DNA strand (γ in Fig. 5) to the coating, which by increasing steric repulsion, offsets both interspecies and intra-species interactions by the same value [see Fig. 6(c) and (d)]. By properly choosing the (high enough) value of $\delta\Delta G^{hy}$ and the density of inter strands, it is possible to cancel the intra-species attraction and keep at the same time a significant interspecies attraction in the temperature window $T_\beta < T < T_\alpha$.

Colloids thus designed, only aggregate in a defined temperature window and the aggregates melt either on cooling or heating, that is, the phase diagram of the binary mixture shows a re-entrant fluid phase.[25] Most important, the system shows a very smooth temperature dependence of the interactions. The result is a substantial extension of the temperature window in which the strength of interspecies attraction is suitable for crystallization.[25]

6 Summary and outlook

Few years after the introduction of DNACCs, the initial enthusiasm about the possibility of using base-pairing interaction to achieve bottom-up assembly of mesoscopic building blocks in complex structures seemed hampered by the complexity of the system. Nevertheless, since then, reliable crystallization strategies of DNA-coated nanocolloids have been developed by more than one group, achieving remarkable control over the crystal structure, the lattice spacing, and other parameters.[16,17,19,20,37,38,47,84,85] However, technological applications such as photonic metamaterials require the same level of control over the assembly of larger building blocks, which seemed to represent an unrealistic target using DNACCs.

In this article we described how experimental, theoretical and computer simulations studies provided a deeper comprehension of the physical effects controlling DNA mediated colloidal interactions, and how new and rationally designed DNA coatings can now be used to facilitate a wider range of self-assembly experiments.

We also reported measurements on colloidal pair-potentials and melting curves that demonstrated the extreme sensitivity of the interactions between micron-sized DNACCs on environmental variables, especially temperature.[10,11,15,27,34,41,42] These findings clarify why in most experimental conditions aggregating colloidal mixtures kinetically arrest in amorphous phases, even though the thermodynamic ground state is expected to be ordered.

We described the most recent theoretical and computer simulation studies that are able to reproduce experimental pair potentials and melting curves and provide an invaluable tool to develop advanced designs for DNA coatings.[10,11,25,26,29,34–36] Important advances recently introduced include are: (i) understanding how length and rigidity of inert-spacers change the entropic component in the hybridization free energy of two sticky ends; (ii) clarifying the role played by the combinatorial entropy following the possibility for one strand to bind to more than a single partner; (iii) introducing the idea of competing linkages to manipulate the temperature dependence of the interactions.

Computer simulations-based studies, already demonstrated that complex coatings with carefully tuned parameters offer the possibility of largely increasing the tendency of micron-sized DNACCs to crystallize.[25] Experimental research groups are presently working to apply the suggested ideas with renewed enthusiasm.

Though general theories, like the one presented by Varilly and coworkers,[33] allow the calculation of pair-potentials for coatings of arbitrary complexity, only a small fraction of this vast parameters-space has been explored so far. By using, for example, more than two competing linkages per colloids, the temperature dependence of DNA mediated interactions could be further manipulated and complex phase diagrams with multiple ordered phases are likely to be observed. Also, very little has been done in studying mixtures with more than two components, or of binary mixtures in which the two species have different sizes or density. Also, DNA mediated assembly of non-spherical colloids is still at its infancy.

Further, more complex scenarios can be investigated by controlling the directionality of DNA-mediated interactions as well as their selectivity and temperature dependence. The surface of the colloids can indeed be patterned in order to graft DNA only on selected patches.[86,87] Recent work by Pine and coworkers demonstrated a strategy to create colloidal analogues of atoms with valence and directional bonding by controlling the number and orientation of DNA patches on the colloid.

The list of possible variations is endless and the newly achieved control over the interactions just opened the door to their investigation.

We conclude this article by suggesting a possible application for DNACCs, which has so far been ignored. Most of the efforts up to this point have been devoted to induce ordered aggregates with lattice spacings on the scale of tens of nanometer up to several micrometer. Amorphous aggregates have often been regarded as unwanted byproducts. However, the investigation

of arrested colloidal phases, that is, gels and glasses, represents one of the hottest areas in soft matter and bio-physics research.[88–90] In our opinion, DNA coated colloids, with the new possibility of precisely controlling the interactions, represent an invaluable tool for the experimental investigation of such poorly understood arrested states of matter. For instance, DNACCs turn out to be excellent gel formers, in which the interaction causing the gelation can be switched on and off almost instantaneously by changing the temperature by a few degrees. Combined with the possibility of building patchy DNACCs, this will allow the experimental investigation of gel-forming ensembles of patchy particles.[90–92]

Moreover, using DNACCs we have the unprecedented possibility of studying multi-component arrested colloidal states, in which the interactions between different components can be designed independently of the others and the morphology (*i.e.* the gels average pore size) can be fully controlled. In collaboration with Foffi and coworkers, we began to explore these possibilities by designing a binary mixture of DNACCs in which intraspecies interactions are strongly attractive whereas inter-species interactions are purely repulsive.[93] Upon cooling below the aggregation temperature, the mixture undergoes an *arrested demixing* leading to the formation of two coexisting, yet spatially independent, colloidal gels. These structures, assembled with isotropic interactions, resemble for example the double-percolating gels found in computer simulations using patchy particles,[91,92] but may also be of relevance in the understanding of protein aggregation on cell membranes.

Beyond the fundamental physical interest in the arrested demixing process, *bigels* and multi-component colloidal gels held together by DNA represent a new whole class of mesoporous materials with potential technological applications in conductive networks, battery manufacture, hybrid semiconductors and photonic band-gap materials. The tip of the iceberg has been sighted – now we need to discover what lies beneath.

Acknowledgements

We acknowledges financial support by the Marie Curie Initial Training Network ITN-COMPLOIDS no. 234810, and the Cavendish Laboratory. We also want to thank D. Frenkel for many fruitful discussions and S. Angioletti-Uberti and P. Varilly for critically reading the manuscript.

References

1 A. P. Alivisatos, K. P. Johnsson, X. Peng, T. E. Wilson, C. J. Loweth, M. P. Bruchez and P. G. Schultz, *Nature*, 1996, **382**, 609–611.
2 C. A. Mirkin, R. L. Letsinger, R. C. Mucic and J. J. Storhoff, *Nature*, 1996, **382**, 607–609.
3 J. Lee, P. Hernandez, J. Lee, A. O. Govorov and N. A. Kotov, *Nat. Mater.*, 2007, **6**, 291–295.
4 F. X. Redl, K. S. Cho, C. B. Murray and S. O'Brien, *Nature*, 2003, **423**, 968–971.
5 J. J. Urban, D. V. Talapin, E. V. Shevchenko, C. R. Kagan and C. B. Murray, *Nat. Mater.*, 2007, **6**, 115–121.
6 J. D. Watson and F. H. C. Crick, *Nature*, 1953, **171**, 737–738.
7 M. H. F. Wilkins, A. R. Stokes and H. R. Wilson, *Nature*, 1953, **171**, 738–740.
8 J. D. Watson and F. H. C. Crick, *Nature*, 1953, **171**, 964–967.
9 N. Geerts and E. Eiser, *Soft Matter*, 2010, **6**, 4647–4660.
10 R. Dreyfus, M. E. Leunissen, R. Sha, A. V. Tkachenko, N. C. Seeman, D. J. Pine and P. M. Chaikin, *Phys. Rev. Lett.*, 2009, **102**, 048301.
11 R. Dreyfus, M. E. Leunissen, R. Sha, A. Tkachenko, N. C. Seeman, D. J. Pine and P. M. Chaikin, *Phys. Rev. E: Stat. Phys., Plasmas, Fluids, Relat. Interdiscip. Top.*, 2010, **81**, 041404.
12 R. Jin, G. Wu, Z. Li, C. A. Mirkin and G. C. Schatz, *J. Am. Chem. Soc.*, 2003, **125**, 1643–1654.
13 J. M. Gibbs-Davis, G. C. Schatz and S. T. Nguyen, *J. Am. Chem. Soc.*, 2007, **129**, 15535–15540.
14 S. Y. Park, J. M. Gibbs-Davis, S. T. Nguyen and G. C. Schatz, *J. Phys. Chem. B*, 2007, **111**, 8785–8791.
15 P. L. Biancaniello, A. J. Kim and J. C. Crocker, *Phys. Rev. Lett.*, 2005, **94**, 058302.
16 S. Y. Park, A. K. R. Lytton-Jean, B. Lee, S. Weigand, G. C. Schatz and C. A. Mirkin, *Nature*, 2008, **451**, 553–556.
17 R. J. Macfarlane, B. Lee, H. D. Hill, A. J. Senesi, S. Seifert and C. A. Mirkin, *Proc. Natl. Acad. Sci. U. S. A.*, 2009, **106**, 10493–10498.
18 P. Cigler, A. K. R. Lytton-Jean, D. G. Anderson, M. G. Finn and S. Y. Park, *Nat. Mater.*, 2010, **9**, 918–922.
19 H. Xiong, D. van der Lelie and O. Gang, *Phys. Rev. Lett.*, 2009, **102**, 015504.
20 D. Nykypanchuk, M. M. Maye, D. van der Lelie and O. Gang, *Nature*, 2008, **451**, 549–552.
21 M. M. Maye, D. Nykypanchuk, D. van der Lelie and O. Gang, *Small*, 2007, **3**, 1678–1682.
22 M. M. Maye, M. T. Kumara, D. Nykypanchuk, W. B. Sherman and O. Gang, *Nat. Nanotechnol.*, 2010, **5**, 116–120.
23 A. J. Kim, P. L. Biancaniello and J. C. Crocker, *Langmuir*, 2006, **22**, 1991–2001.
24 A. J. Kim, R. Scarlett, P. L. Biancaniello, T. Sinno and J. C. Crocker, *Nat. Mater.*, 2009, **8**, 52–55.
25 S. Angioletti-Uberti, B. M. Mognetti and D. Frenkel, *Nat. Mater.*, 2012, **11**, 518–522.
26 B. M. Mognetti, M. E. Leunissen and D. Frenkel, *Soft Matter*, 2012, **8**, 2213–2221.
27 M. E. Leunissen, R. Dreyfus, R. Sha, N. C. Seeman and P. M. Chaikin, *J. Am. Chem. Soc.*, 2010, **132**, 1903–1913.
28 F. J. Martinez-Veracoechea, B. M. Mladek, A. V. Tkachenko and D. Frenkel, *Phys. Rev. Lett.*, 2011, **107**, 045902.
29 M. E. Leunissen and D. Frenkel, *J. Chem. Phys.*, 2011, **134**, 084702.
30 N. A. Licata and A. V. Tkachenko, *Phys. Rev. E: Stat. Phys., Plasmas, Fluids, Relat. Interdiscip. Top.*, 2006, **74**, 041408.

31 N. A. Licata and A. V. Tkachenko, *Phys. Rev. E: Stat. Phys., Plasmas, Fluids, Relat. Interdiscip. Top.*, 2006, **74**, 041406.
32 A. V. Tkachenko, *Phys. Rev. Lett.*, 2002, **89**, 148303.
33 P. Varilly, S. Angioletti-Uberti, B. M. Mognetti and D. Frenkel, *J. Chem. Phys.*, 2012, **137**, 094108.
34 W. B. Rogers and J. C. Crocker, *Proc. Natl. Acad. Sci. U. S. A.*, 2011, **108**, 15687–15692.
35 B. M. Mognetti, P. Varilly, S. Angioletti-Uberti, F. J. Martinez-Veracoechea, J. Dobnikar, M. E. Leunissen and D. Frenkel, *Proc. Natl. Acad. Sci. U. S. A.*, 2012, **109**, E378–E379.
36 W. B. Rogers and J. C. Crocker, *Proc. Natl. Acad. Sci. U. S. A.*, 2012, **109**, E380.
37 T. A. Taton, G. Lu and C. A. Mirkin, *J. Am. Chem. Soc.*, 2001, **123**, 5164–5165.
38 S. J. Hurst, H. D. Hill and C. A. Mirkin, *J. Am. Chem. Soc.*, 2008, **130**, 12192–12200.
39 T. A. Taton, C. A. Mirkin and R. L. Letsinger, *Science*, 2000, **289**, 1757–1760.
40 S.-J. Park, T. A. Taton and C. A. Mirkin, *Science*, 2002, **295**, 1503–1506.
41 M. E. Leunissen, R. Dreyfus, R. Sha, T. Wang, N. C. Seeman, D. J. Pine and P. M. Chaikin, *Soft Matter*, 2009, **5**, 2422–2430.
42 M. E. Leunissen, R. Dreyfus, F. C. Cheong, D. G. Grier, R. Sha, N. C. Seeman and P. M. Chaikin, *Nat. Mater.*, 2009, **8**, 590–595.
43 A. Holmberg, A. Blomstergren, O. Nord, M. Lukacs, J. Lundeberg and M. Uhlén, *Electrophoresis*, 2005, **26**, 501–510.
44 B. Tinland, A. Pluen, J. Sturm and G. Weill, *Macromolecules*, 1997, **30**, 5763–5765.
45 S. Brinkers, H. R. C. Dietrich, F. H. de Groote, I. T. Young and B. Rieger, *J. Chem. Phys.*, 2009, **130**, 215105.
46 R. J. Macfarlane, M. R. Jones, A. J. Senesi, K. L. Young, B. Lee, J. Wu and C. A. Mirkin, *Angew. Chem., Int. Ed.*, 2010, **49**, 4589–4592.
47 H. D. Hill, R. J. Macfarlane, A. J. Senesi, B. Lee, S. Y. Park and C. A. Mirkin, *Nano Lett.*, 2008, **8**, 2341–2344.
48 T. Yanagishima, L. Di Michele, J. Kotar and E. Eiser, *Soft Matter*, 2012, **8**, 6792–6798.
49 R. J. Macfarlane, B. Lee, M. R. Jones, N. Harris, G. C. Schatz and C. A. Mirkin, *Science*, 2011, **334**, 204–208.
50 O. Padovan-Merhar, F. Vargas Lara and F. W. Starr, *J. Chem. Phys.*, 2011, **134**, 244701.
51 F. Vargas Lara and F. W. Starr, *Soft Matter*, 2011, **7**, 2085–2093.
52 F. W. Starr and F. Sciortino, *J. Phys.: Condens. Matter*, 2006, **18**, L347.
53 W. Dai, C. W. Hsu, F. Sciortino and F. W. Starr, *Langmuir*, 2009, **26**, 3601–3608.
54 C. W. Hsu, J. Largo, F. Sciortino and F. W. Starr, *Proc. Natl. Acad. Sci. U. S. A.*, 2008, **105**, 13711–13715.
55 M. V. Satish Kumar and P. K. Maiti, *Soft Matter*, 2012, **8**, 1893–1900.
56 B. M. Mladek, J. Fornleitner, F. J. Martinez-Veracoechea, A. Dawid and D. Frenkel, *Phys. Rev. Lett.*, 2012, **108**, 268301.
57 B. Bozorgui and D. Frenkel, *Phys. Rev. Lett.*, 2008, **101**, 045701.
58 F. J. Martinez-Veracoechea, B. Bozorgui and D. Frenkel, *Soft Matter*, 2010, **6**, 6136–6145.
59 C. Knorowski, S. Burleigh and A. Travesset, *Phys. Rev. Lett.*, 2011, **106**, 215501.
60 T. I. N. G. Li, R. Sknepnek, R. J. Macfarlane, C. A. Mirkin and M. Olvera de la Cruz, *Nano Lett.*, 2012, **12**, 2509–2514.
61 C. W. Hsu, F. Sciortino and F. W. Starr, *Phys. Rev. Lett.*, 2010, **105**, 055502.
62 T. E. Ouldridge, A. A. Louis and J. P. K. Doye, *J. Chem. Phys.*, 2011, **134**, 085101.
63 P. Sulc, F. Romano, T. E. Ouldridge, L. Rovigatti, J. P. K. Doye and A. A. Louis, *J. Chem. Phys.*, 2012, **137**, 135101.
64 O.-S. Lee, V. Y. Cho and G. C. Schatz, *J. Phys. Chem. B*, 2012, **116**, 7000–7005.
65 O.-S. Lee and G. C. Schatz, *in Computational Studies of the Properties of DNA-Linked Nanomaterials*, John Wiley & Sons, Inc., 2012, pp. 197–249.
66 O.-S. Lee, T. R. Prytkova and G. C. Schatz, *J. Phys. Chem. Lett.*, 2010, **1**, 1781–1788.
67 H. D. Hill, J. E. Millstone, M. J. Banholzer and C. A. Mirkin, *ACS Nano*, 2009, **3**, 418–424.
68 P. H. Rogers, E. Michel, C. A. Bauer, S. Vanderet, D. Hansen, B. K. Roberts, A. Calvez, J. B. Crews, K. O. Lau, A. Wood, D. J. Pine and P. V. Schwartz, *Langmuir*, 2005, **21**, 5562–5569.
69 V. T. Milam, A. L. Hiddessen, J. C. Crocker, D. J. Graves and D. A. Hammer, *Langmuir*, 2003, **19**, 10317–10323.
70 S. Jahn, N. Geerts and E. Eiser, *Langmuir*, 2010, **26**, 16921–16927.
71 N. Geerts and E. Eiser, *Soft Matter*, 2010, **6**, 664–669.
72 N. Geerts, S. Jahn and E. Eiser, *J. Phys.: Condens. Matter*, 2010, **22**, 104111.
73 J. C. Crocker, J. A. Matteo, A. D. Dinsmore and A. G. Yodh, *Phys. Rev. Lett.*, 1999, **82**, 4352–4355.
74 M.-P. Valignat, O. Theodoly, J. C. Crocker, W. B. Russel and P. M. Chaikin, *Proc. Natl. Acad. Sci. U. S. A.*, 2005, **102**, 4225–4229.
75 A. Singh, H. Eksiri and Y. G. Yingling, *J. Polym. Sci., Part B: Polym. Phys.*, 2011, **49**, 1563–1568.
76 J. SantaLucia, *Proc. Natl. Acad. Sci. U. S. A.*, 1998, **95**, 1460–1465.
77 D. Frenk and B. Smit, *Understanding Molecular Simulations*, Academic Press, San Diego, CA, 2002.
78 S. Angioletti-Uberti, P. Varilly, B. M. Mognetti, A. V. Tkachenko and D. Frenkel, *J. Chem. Phys.*, 2013, **138**, 021102.
79 D. B. Lukatsky and D. Frenkel, *Phys. Rev. Lett.*, 2004, **92**, 068302.
80 D. B. Lukatsky and D. Frenkel, *J. Chem. Phys.*, 2005, **122**, 214904.
81 D. B. Lukatsky, B. M. Mulder and D. Frenkel, *J. Phys.: Condens. Matt.*, 2006, **18**, S567–S580.
82 R. P. Sear, *Mol. Phys.*, 1997, **107**, 7477.
83 O. Gang, *Nat. Mater.*, 2012, **11**, 487–488.

84 C. Chi, F. Vargas-Lara, A. V. Tkachenko, F. W. Starr and O. Gang, *ACS Nano*, 2012, **6**, 6793–6802.
85 R. C. Mucic, J. J. Storhoff, C. A. Mirkin and R. L. Letsinger, *J. Am. Chem. Soc.*, 1998, **120**, 12674–12675.
86 L. Hong, A. Cacciuto, E. Luijten and S. Granick, *Langmuir*, 2008, **24**, 621–625.
87 Y. Wang, Y. Wang, D. R. Breed, V. N. Manoharan, L. Feng, A. D. Hollingsworth, M. Weck and D. J. Pine, *Nature*, 2012, **491**, 51–55.
88 P. J. Lu, E. Zaccarelli, F. Ciulla, A. B. Schofield, F. Sciortino and D. A. Weitz, *Nature*, 2008, **453**, 499–503.
89 E. Zaccarelli, *J. Phys.: Condens. Matter*, 2007, **19**, 323101.
90 F. Sciortino and E. Zaccarelli, *Curr. Opin. Solid State Mater. Sci.*, 2011, **15**, 246–253.
91 D. de las Heras, J. M. Tavares and M. M. Telo da Gama, *Soft Matter*, 2012, **8**, 1785–1794.
92 A. Goyal, C. K. Hall and O. D. Velev, *Soft Matter*, 2010, **6**, 480–484.
93 F. Varrato, L. Di Michele, M. Belushkin, N. Dorsaz, S. H. Nathan, E. Eiser and G. Foffi, *Proc. Natl. Acad. Sci. U. S. A.*, 2012, **109**, 19155–19160.